

Temporal Correlation of Interference in Wireless Networks with Rayleigh Block Fading

Udo Schilcher, *Student Member, IEEE*, Christian Bettstetter, *Senior Member, IEEE*, and Günther Brandner, *Student Member, IEEE*

Abstract—The temporal correlation of interference is a key performance factor of several technologies and protocols for wireless communications. A comprehensive understanding of interference correlation is especially important in the design of diversity schemes, whose performance can severely degrade in case of highly-correlated interference. Taking into account three sources of correlation—node locations, channel, and traffic—and using common modeling assumptions—random homogeneous node positions, Rayleigh block fading, and slotted ALOHA traffic—we derive closed-form expressions and calculation rules for the correlation coefficient of the overall interference power received at a certain point in space. Plots give an intuitive understanding as to how model parameters influence the interference correlation.

Index Terms—Wireless networks, interference, correlation, Rayleigh fading, spatial stochastics, time diversity.

1 INTRODUCTION AND MOTIVATION

MOBILE communication systems have to cope with the fact that the quality of a radio link varies over time. Such time-variant behavior of the wireless environment is mainly caused by two factors. First, mobility of devices and obstacles changes the multipath propagation constellation. These changes lead to fluctuations of the received signal power over time (fading). Second, the data traffic sent by devices and base stations varies over time, which in turn changes the interference situation and leads to fluctuations of the signal-to-interference ratio at a given receiver.

Several communication techniques and protocols actually exploit this time-varying behavior. The basic idea is as follows: if a transmission fails at a certain time instant, it might well succeed at a later time instant. Methods using this approach include pure time diversity schemes—e.g., retransmission protocols [1], channel coding with interleaving [2]—and space-time diversity schemes—e.g., space-time coding [3], cooperative relaying [4], and opportunistic scheduling [5]. The implementation of such schemes requires a comprehensive understanding of the temporal autocorrelation of the received signal. Informally speaking, the correlation indicates what difference to expect between two signal samples, i.e., how well can one value be estimated when knowing the other. Applied to wireless communications, the temporal correlation of a signal tells us how long to wait until the environment's characteristics change significantly, such

that a retransmission makes sense.

The correlation of a *signal* suffering from channel fading has been investigated in detail by real-world measurements and mathematical models (see, e.g., [6]–[8] and references therein). Such work considers a point-to-point link, e.g., between a mobile computer and a base station. An important parameter in this context is the channel coherence time, which quantifies the period over which signal values are likely to experience comparable attenuation. Messages separated by a time span much longer than the coherence time have little to no correlation and are thus expected to experience different fading conditions.

The correlation of *interference* has received much less attention in the literature, despite the fact that it also has significant impact on system design and performance. This kind of analysis must consider multipoint-to-point communications, such as a shared link between several mobile devices and a base station. Profound knowledge of this domain is needed to optimize protocols and improve performance. First analytical results toward a better understanding of interference correlation were recently achieved by Haenggi and Ganti (see [9]–[11]). We continue their work by analyzing the temporal correlation of interference on a broader set of scenarios, accounting for a larger set of causes for correlation.

The contributions of this article are as follows: We investigate temporal correlation of the overall interference power at a certain point in space obtained for various modeling assumptions. Hereby, we consider three main reasons that may cause interference correlation:

- i) the node locations are temporarily correlated,
- j) the wireless channel shows a temporal correlation,
- k) the traffic sent by nodes is temporarily correlated.

Each of these system properties is modeled in three ways (see Section 2). All 27 combinations of reasons

• The authors are with the Institute of Networked and Embedded Systems, Lakeside B02, University of Klagenfurt, Austria.
E-mail: see <http://nes.aau.at>

• C. Bettstetter is also with Lakeside Labs GmbH, Klagenfurt, Austria.

Manuscript received September 7, 2010; revised April 20 and September 6, 2011.

and modeling assumptions are considered, where each of them is denoted by a triple $(i, j, k) \in \{0, 1, 2\}^3$. For each case (i, j, k) , we analyze the temporal correlation of interference by means of the correlation coefficient (Section 3). In fact, the article provides closed-form expressions of correlation coefficients and their limiting distributions for randomly homogeneously positioned nodes, Rayleigh block fading, and Poisson-like traffic resulting from slotted ALOHA. Interpretation of the results leads to a better understanding of the influence of message arrival rate, channel coherence time, and message length on interference correlation.

2 MODELING ASSUMPTIONS

The covariance between two random variables X_1 and X_2 with expected values $\mathbb{E}[X_1]$ and $\mathbb{E}[X_2]$ is given by

$$\text{cov}(X_1, X_2) = \mathbb{E}[X_1 X_2] - \mathbb{E}[X_1] \cdot \mathbb{E}[X_2]. \quad (1)$$

Informally speaking, it is a measure for the relationship between the two variables. If the covariance is positive (negative), high values for one variable imply high values (low values) for the other. If the covariance is zero, there is no linear relationship between the two variables.

The correlation between two random variables is measured in terms of a normalized covariance, namely by Pearson's correlation coefficient [12]

$$\rho(X_1, X_2) := \frac{\text{cov}(X_1, X_2)}{\sqrt{\text{var}(X_1)}\sqrt{\text{var}(X_2)}} \quad (2)$$

with $\rho \in [-1, +1]$. The two variables are fully positively correlated if $\rho = +1$ and fully negatively correlated if $\rho = -1$. They are uncorrelated if $\rho = 0$. Independent random variables are always uncorrelated.

Time is discretized into slots of equal durations; these slots are indexed by $\tau \in \mathbb{N}$. The objective of this article is to derive, for each case (i, j, k) , the correlation coefficient $\rho(i, j, k)$ of the received interference power in two consecutive time slots $\tau = t - 1$ and t .

2.1 Node Locations

The network nodes are distributed on the plane \mathbb{R}^2 using a Poisson point process with intensity λ . A set of node locations is denoted by \mathcal{N} . We consider three options:

- 0) *Static*. The locations \mathcal{N} remain fixed over all time slots. They are a given condition under which the interference analysis is performed.
- 1) *Randomly changing*. The locations \mathcal{N} are chosen anew in each slot, independent of previous slots, by a realization of the Poisson process.
- 2) *Static but unknown*. The locations \mathcal{N} remain fixed over all slots but they are unknown. The interference analysis is conducted over the population of all possible locations. A spatial average is taken over all realizations of the Poisson point process (cf. [10]).

The distance of a node location $x \in \mathcal{N}$ to the origin $(0, 0)$ is denoted by $\|x\|$ normalized to meters.

2.2 Channel

Each node has the same transmit power κ . The wireless channel is modeled with a distance-dependent path loss and Rayleigh fading caused by multipath propagation. We are interested in the overall power received at a given point in space. Without loss of generality, due to the stationarity of the Poisson point process, we consider the received power at the origin $(0, 0)$ of the plane \mathbb{R}^2 .

The power received from node x is denoted by the random variable $I(x)$. It can be expressed by [13]

$$I(x) := \kappa \cdot l(\|x\|) \cdot h_x^2. \quad (3)$$

The term $l(\|x\|)$ is the path loss function describing the power attenuation over distance; it is typically modeled by $l(\|x\|) := \min(1, \|x\|^{-\alpha})$ with path loss exponent $\alpha \geq 2$. The term h_x is a random variable that models the effects of multipath fading; it is independent from node to node [14]. A generalized block fading channel is applied, in which the channel state does not change during c consecutive time slots and then changes to an independent random value (also see [9], [15], [16]). The value $1/c$ is a measure for the rapidity of fading.

The channel is modeled in three different ways:

- 0) *Deterministic and constant*. The overall attenuation for a given distance is constant over time (no fading, i.e. $h_x \equiv 1$).
- 1) *Randomly changing each slot*. The overall attenuation for a given distance varies randomly over time according to Rayleigh fading with $c = 1$, i.e. the channel state is independent from slot to slot.
- 2) *Randomly changing each c slots*. The overall attenuation for a given distance varies randomly over time according to Rayleigh fading with $c \geq 2$. This introduces dependencies in the channel states.

In Cases 1 and 2, the fading state h_x^2 is an exponentially distributed random variable with expected value $\mathbb{E}[h_x^2] = \mu = 1$, i.e., it comprises the probability density $f_{h_x^2}(\xi) = 1/\mu \cdot \exp(-\xi/\mu) = \exp(-\xi)$. The same channel model (Case 0 and 1) was used in a related study [11].

The expected value of the reception power with respect to fading for a fixed node location x is given by

$$\mathbb{E}[I(x) | x] = I(x)|_{h_x=1} = \kappa \cdot l(\|x\|). \quad (4)$$

Note that the expected values $\mathbb{E}[I(x) | x]$ generally differ, as the distances $\|x\|$ between the interfering nodes and the origin usually vary.

2.3 Traffic

Slotted ALOHA [17] is employed for medium access control. All messages have the same duration of d slots. Some nodes are randomly selected to act as senders; this subset of nodes is called \mathcal{S} ; the fraction of nodes from \mathcal{N} in \mathcal{S} is called $S \in [0, 1]$. The nonsending nodes $\mathcal{N} \setminus \mathcal{S}$ are called idle nodes. A given node is modeled in three different ways:

- 0) *Constant*. At the beginning, each node decides whether to become sender or idle node. A node

becomes sender with probability p and keeps its role for the entire time. Each sender transmits in each slot with probability one.

- 1) *Randomly changing each slot.* The decision of a node to become sender or not is made anew in each slot and independently of previous slots. It becomes sender with probability p . The message duration is $d = 1$ slot.
- 2) *Randomly changing with message length d .* The set of senders \mathcal{S} again changes over time. The message duration exceeds one slot ($d \geq 2$). In each slot, each idle node starts sending with probability $\frac{p}{1-p(d-1)}$. This probability is chosen such that an expected fraction p of all nodes start sending a message within each slot. Note that we have to ensure $dp \leq 1$. The expected fraction of nodes sending at a given time instant is thus $S = dp$. This model introduces dependencies in the traffic.

3 TEMPORAL CORRELATION OF INTERFERENCE

All signals radiated by senders are regarded as interference at the origin. The instantaneous value of the overall interference power $I(\mathcal{S})$ caused by the senders \mathcal{S} in a given time slot is the sum [11]

$$I(\mathcal{S}) := \sum_{x \in \mathcal{S}} I(x) \stackrel{(3)}{=} \sum_{x \in \mathcal{S}} \kappa \cdot l(\|x\|) \cdot h_x^2. \quad (5)$$

As mentioned above, we consider the overall interference $I(\mathcal{S})$ at two consecutive time slots and derive the correlation coefficient ρ between these two interference values according to (2). Table 1 summarizes the results for all possible cases $(i, j, k) \in \{0, 1, 2\}^3$. All results have been backed up by computer simulations. These are shown for the first nontrivial case $(0, 0, 2)$ but are omitted in all further cases, as they would not provide any additional information.

Let us make some definitions that will subsequently be useful. As the set of senders \mathcal{S} in general changes over time, we use an indicator variable $\gamma_x(\mathcal{S})$ denoting whether or not a node $x \in \mathcal{N}$ is contained in \mathcal{S} , i.e.,

$$\gamma_x(\mathcal{S}) := \begin{cases} 1 & x \in \mathcal{S} \\ 0 & \text{else.} \end{cases} \quad (6)$$

This variable is Bernoulli distributed with variance

$$\text{var}(\gamma_x(\mathcal{S})) = \mathbb{E}[S] (1 - \mathbb{E}[S]). \quad (7)$$

It can be exploited to express the interference as

$$I(\mathcal{S}) = \sum_{x \in \mathcal{S}} I(x) = \sum_{x \in \mathcal{N}} \kappa \cdot l(\|x\|) \cdot h_x^2 \cdot \gamma_x(\mathcal{S}). \quad (8)$$

TABLE 1
Correlation of Interference: Summary of Results

Locations	Channel	Traffic	Interference	Eq.
i	j	k	ρ	
0	0	0	undefined	
0	0	1	0	
0	0	2	$\frac{(d-1)(dp-1)}{d(p(d-1)-1)}$	(29)
0	1	0	0	
0	1	1	0	
0	1	2	$\frac{(d-1)(dp-1)^2}{d(p(d-1)-1)(dp-2)}$	(33)
0	2	0	$\frac{c-1}{c}$	(43)
0	2	1	$\frac{p(1+p(c-2))}{(2-p)(1+p(c-1))}$	(49)
0	2	2	-	(61)
1	0, 1, or 2	0, 1, or 2	0	
2	0	0	1	(13)
2	0	1	p	(11)
2	1	0	$1/2$	(14)
2	1	1	$p/2$	(12)
2	0, 1	2	$\frac{d-1+p/(1-p(d-1))}{d \mathbb{E}[h^4]}$	(42)
2	2	0	$\frac{2c-1}{2c}$	(44)
2	2	1	$\frac{p}{2} \left(2 - \frac{p}{1+p(c-1)} \right)$	(47)
2	2	2	-	(64)

The expected interference in a given slot is [10]

$$\begin{aligned} \mathbb{E}[I(\mathcal{S})] &\stackrel{(5)}{=} \mathbb{E} \left[\sum_{x \in \mathcal{S}} \kappa \cdot l(\|x\|) \cdot h_x^2 \right] \\ &= \kappa \cdot \mathbb{E} \left[\sum_{x \in \mathcal{S}} l(\|x\|) \right] \\ &= \kappa \cdot dp\lambda \cdot \int_{\mathbb{R}^2} l(\|x\|) dx \quad (9) \\ &\stackrel{\alpha \geq 2}{=} \kappa \cdot dp\lambda \cdot \frac{\alpha\pi}{\alpha-2}. \quad (10) \end{aligned}$$

The second equality holds as κ is constant, the random variables $l(\|x\|)$ and h_x^2 are independent of each other, and $\mathbb{E}[h_x^2] \equiv 1$. The third equality holds due to Campbell's theorem (Chapter 10.2 in [12]) and because the density of sending nodes is $dp\lambda$. The resulting integral converges for the practically relevant case $\alpha > 2$.

It is useful to classify all senders of two consecutive time slots into three disjoint sets: Nodes sending in both slots are assigned to set \mathcal{S}_{11} . Nodes sending in the first slot only are in set \mathcal{S}_{10} . And nodes sending in the second slot only are in set \mathcal{S}_{01} . The set \mathcal{S}_{11} can be further subdivided into two disjoint sets: Nodes occupying both slots with the same message are called \mathcal{S}_{11}^* . Nodes that finish a message transmission in the first slot and start a new message in the second slot are called \mathcal{S}_{11}^{**} . Clearly, $\mathcal{S}_{11} = \mathcal{S}_{11}^* \cup \mathcal{S}_{11}^{**}$. Similarly, senders experiencing the same channel state in both slots are called \mathcal{S}'_{11} , and senders with different channel states in these slots are called \mathcal{S}''_{11} . Let S_{11} denote the fraction of nodes within \mathcal{S}_{11} and use a similar notation for all other sets.

Appendix A provides two theorems on the correlation between interference values from disjoint node sets, which will be used in the following derivations.

3.1 The Nonrandom Case (0, 0, 0).

The only case where no randomness occurs is $(i, j, k) = (0, 0, 0)$. The variance of the interference is zero since the interference value remains constant over all time slots. Hence, the correlation coefficient $\rho(0, 0, 0)$ is not defined.

3.2 The Cases without Correlation; Cases (0, 0, 1), (0, 1, 0), and (0, 1, 1).

If all node locations are fixed ($i = 0$), correlation of two interference values can arise from channel or traffic correlation. If $j, k \in \{0, 1\}$ with $j + k > 0$ no source of correlation exists; thus we always have $\rho(0, j, k) = 0$.

3.3 Correlation for Randomly Changing Node Positions; Cases (1, j, k).

All scenarios in which the node locations are statistically independent for each slot can be analyzed collectively. Even if dependencies in channel and traffic exist, these dependencies show no effect due to the new random position of all nodes. The correlation of interference for all these cases is zero, i.e., $\rho(1, j, k) = 0 \forall j, k \in \{0, 1, 2\}$. Note that case $(1, 0, k)$ is unrealistic, as it assumes a constant channel with randomly changing node positions.

3.4 Correlation Caused by Node Positions; Cases (2, j, k) with $j, k \in \{0, 1\}$.

The implications of correlated node locations on interference have been investigated by Haenggi and Ganti (see [10], [11]). That work covers the cases $(2, 0, 1)$ and $(2, 1, 1)$ in our notation. Results (Corollary 2 in [10]) state that

$$\rho(2, 0, 1) = p \quad \text{and} \quad (11)$$

$$\rho(2, 1, 1) = \frac{p}{2}. \quad (12)$$

They can be applied to the following cases: In case $(2, 0, 0)$, always the same nodes transmit in each slot. Idle nodes can be neglected, resulting in the same correlation as in case $(2, 0, 1)$ with sending probability $p = 1$, i.e.

$$\rho(2, 0, 0) = 1. \quad (13)$$

Similarly, case $(2, 1, 0)$ can be derived from $(2, 1, 1)$ by setting $p = 1$, leading to

$$\rho(2, 1, 0) = \frac{1}{2}. \quad (14)$$

3.5 Correlation Caused by Traffic; Cases (0, 0, 2) and (0, 1, 2).

If messages exceed one slot, a positive correlation of the interference in two consecutive slots is introduced. Let us subdivide all senders into different sets as explained above. We are interested in the correlation coefficient between interference caused by nodes sending in the first slot ($\mathcal{S}_{11} \cup \mathcal{S}_{10}$) and interference caused by nodes sending in the second slot ($\mathcal{S}_{11} \cup \mathcal{S}_{01}$). We have

$$\rho(0, j, 2) = \frac{\mathbb{E}[\text{cov}(I(\mathcal{S}_{11} \cup \mathcal{S}_{10}), I(\mathcal{S}_{11} \cup \mathcal{S}_{01}) | \mathcal{N})]}{\mathbb{E}[\text{var}(I(\mathcal{S}) | \mathcal{N})]} \quad (15)$$

with $I(\mathcal{S}_{11} \cup \mathcal{S}_{10}) = I(\mathcal{S}_{11}) + I(\mathcal{S}_{10})$ and $I(\mathcal{S}_{11} \cup \mathcal{S}_{01}) = I(\mathcal{S}_{11}) + I(\mathcal{S}_{01})$. The following paragraphs derive the enumerator and denominator of this expression. For simplicity of notation, we use the abbreviations $I_{11} := I(\mathcal{S}_{11})$, $I_{10} := I(\mathcal{S}_{10})$, and $I_{01} := I(\mathcal{S}_{01})$.

The enumerator of (15) expands to

$$\begin{aligned} \mathbb{E}[\text{cov}(I_{11} + I_{10}, I_{11} + I_{01} | \mathcal{N})] &= \\ &= \mathbb{E}[\text{var}(I_{11} | \mathcal{N})] + 2\mathbb{E}[\text{cov}(I_{11}, I_{10} | \mathcal{N})] \\ &+ \mathbb{E}[\text{cov}(I_{10}, I_{01} | \mathcal{N})]. \end{aligned} \quad (16)$$

The covariances in this expression can be computed by rearranging (2) to

$$\begin{aligned} \mathbb{E}[\text{cov}(I_{10}, I_{01} | \mathcal{N})] &= \\ &= \rho(I_{10}, I_{01}) \cdot \sqrt{\mathbb{E}[\text{var}(I_{10} | \mathcal{N})]} \sqrt{\mathbb{E}[\text{var}(I_{01} | \mathcal{N})]} \end{aligned} \quad (17)$$

and similar for $\mathbb{E}[\text{cov}(I_{11}, I_{10} | \mathcal{N})]$.

To compute the two correlation coefficients, we must know the expected fractions of nodes in the three sender sets. For this reason, we also use the subsets \mathcal{S}_{11}^* and \mathcal{S}_{11}^{**} . The nodes \mathcal{S}_{11}^* occupy both slots with one message. These nodes start a message in slot $t - (d - 1), \dots, t - 2$, or $t - 1$. The fraction of nodes contained in this set is $S_{11}^* = p(d - 1)$. The nodes \mathcal{S}_{11}^{**} start messages in slots $t - d$ and t . Their fraction is $S_{11}^{**} = \frac{p^2}{1 - p(d - 1)}$.

The expected fraction of nodes in \mathcal{S}_{11} is thus

$$\mathbb{E}[S_{11}] = p(d - 1) + \frac{p^2}{1 - p(d - 1)}. \quad (18)$$

Since, in each slot, a fraction p of all nodes start a message, we have

$$\mathbb{E}[S_{10}] = \mathbb{E}[S_{01}] = p - \frac{p^2}{1 - p(d - 1)}. \quad (19)$$

3.5.1 Constant channel

If no fading is present, we apply (18) and (19) in Theorem 1 of Appendix A to obtain

$$\rho(I_{10}, I_{11}) = -\sqrt{\frac{p^2(1 - d + pd(d - 2))}{(p(d - 2) - 1)(p^2d - pd + 1)}} \quad (20)$$

$$\text{and } \rho(I_{10}, I_{01}) = -\frac{p(dp - 1)}{dp(p - 1) + 1}. \quad (21)$$

Let $\gamma_x(\mathcal{S}_{10})$ denote the indicator variable that node $x \in \mathcal{S}_{10}$. It is Bernoulli distributed with variance

$$\text{var}(\gamma_x(\mathcal{S}_{10})) = \mathbb{E}[S_{10}] (1 - \mathbb{E}[S_{10}]). \quad (22)$$

The indicator variables $\gamma_x(\mathcal{S}_{01})$, $\gamma_x(\mathcal{S}_{11})$, and $\gamma_x(\mathcal{S})$ are defined in a similar manner.

The expected variance of the interference caused by the nodes \mathcal{S}_{10} for given node locations \mathcal{N} is

$$\begin{aligned} \mathbb{E}[\text{var}(I_{10} | \mathcal{N})] &= \mathbb{E} \left[\text{var} \left(\sum_{x \in \mathcal{N}} \kappa l(\|x\|) \gamma_x(\mathcal{S}_{10}) \mid \mathcal{N} \right) \right] \\ &= \kappa^2 \cdot \mathbb{E} \left[\sum_{x \in \mathcal{N}} l^2(\|x\|) \right] \cdot \text{var}(\gamma_x(\mathcal{S}_{10})) \end{aligned} \quad (23)$$

$$= \kappa^2 \cdot \lambda \int_{\mathbb{R}^2} l^2(\|x\|) dx \cdot \frac{p(dp-1)(dp^2-dp+1)}{(p(d-1)-1)^2} \quad (24)$$

$$\stackrel{\alpha \geq 2}{=} \kappa^2 \cdot \lambda \frac{\alpha\pi}{\alpha-1} \cdot \frac{p(dp-1)(dp^2-dp+1)}{(p(d-1)-1)^2}. \quad (25)$$

These equations hold since κ and $l(\|x\|)$ are constants regarding the variance operator, because the sum can be converted to an integral using Campbell's theorem, and because we apply (22) with (19) in (23). The same expression is obtained for the interference caused by \mathcal{S}_{01} . The expression for \mathcal{S}_{11} is obtained using $\mathbb{E}[S_{11}]$ according to (18) instead of $\mathbb{E}[S_{10}]$ in (22), and applying the resulting variance in (23).

We have now all terms to compute (17) and related expressions, which can in turn be used to compute (16).

The denominator of (15) without fading is

$$\begin{aligned} \mathbb{E}[\text{var}(I(\mathcal{S}) | \mathcal{N})] &\stackrel{(8)}{=} \mathbb{E} \left[\text{var} \left(\sum_{x \in \mathcal{N}} \kappa l(\|x\|) \gamma_x(\mathcal{S}) \mid \mathcal{N} \right) \right] \\ &= \kappa^2 \cdot \mathbb{E} \left[\sum_{x \in \mathcal{N}} l^2(\|x\|) \right] \cdot \text{var}(\gamma_x(\mathcal{S})) \end{aligned} \quad (26)$$

$$= \kappa^2 \cdot \lambda \int_{\mathbb{R}^2} l^2(\|x\|) dx \cdot dp(1-dp) \quad (27)$$

$$\stackrel{\alpha \geq 2}{=} \kappa^2 \cdot \lambda \frac{\alpha\pi}{\alpha-1} \cdot dp(1-dp). \quad (28)$$

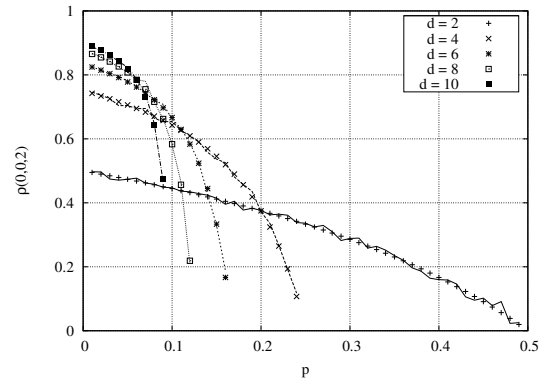
The third equality holds due to Campbell's theorem with node density λ and due to (7) with $\mathbb{E}[S] = dp$.

The resulting correlation coefficient is

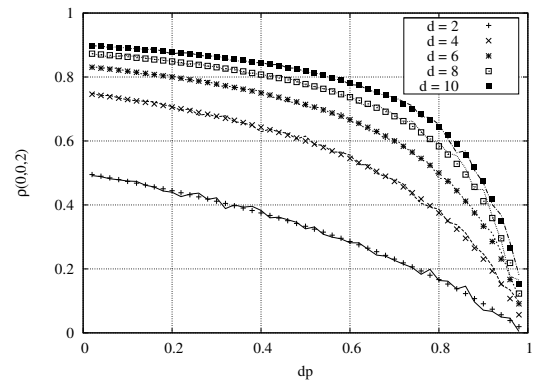
$$\rho(0, 0, 2) = \frac{(16)}{(28)} = \frac{(d-1)(dp-1)}{d(p(d-1)-1)} \quad (29)$$

independent of κ , λ , and α . Figure 1 presents a plot of $\rho(0, 0, 2)$ for different values of the sending probability p and message duration d . Marks indicate the values obtained from the mathematical expression. Lines show results from simulations carried out as a validity check using $\kappa = 1$ mW, $\lambda = 10^{-4}$, and $\alpha = 3$. The simulations fully support the analytical results. Simulations were performed over 10,000 slots, where each pair of consecutive slots was considered. The experiment was repeated 10 times, and results were averaged over these runs.

As shown in Figure 1(a), the interference correlation decreases with an increasing fraction p of senders for a given message duration. The curves end at $pd = 1$, where no correlation exists. For high p -values, almost all nodes are sending, and thus each node is either in \mathcal{S}_{10}



(a) Plot of $\rho(0, 0, 2)$ over p .



(b) Plot of $\rho(0, 0, 2)$ over dp .

Fig. 1. Interference correlation in case $(0, 0, 2)$. Points are analytical results and lines are simulation results.

or \mathcal{S}_{11} in the first slot, while nodes are interchanging between these sets. This causes a high negative correlation $\rho(I_{10}, I_{11})$, which in turn decreases $\rho(0, 0, 2)$.

Figure 1(b) shows the correlation coefficient over the expected fraction of sending nodes $S = dp$. For given p , the correlation increases with the message duration d . This behavior results from the fact that the message duration is an indicator for the fraction of nodes sending in both slots, and nodes sending in both slots lead to interference correlation. The correlation coefficient approaches one in the limit, i.e., $\lim_{d \rightarrow \infty} \rho(0, 0, 2) = 1$, where $dp \leq 1$ needs to be ensured, which implies $p \rightarrow 0$.

3.5.2 Channel changing randomly each slot

Let us now turn to a channel that changes each slot with Rayleigh fading and derive the numerator and denominator of (15) in this case as well. It follows from Theorem 2 in Appendix A that fading does not influence the numerator $\text{cov}(I(\mathcal{S}_{11} \cup \mathcal{S}_{10}), I(\mathcal{S}_{11} \cup \mathcal{S}_{01}) | \mathcal{N})$. The denominator—the expected variance of the overall interference for given locations—is given by (cp. (26))

$$\mathbb{E}[\text{var}(I(\mathcal{S}) | \mathcal{N})] = \kappa^2 \cdot \lambda \int_{\mathbb{R}^2} l^2(\|x\|) dx \cdot \text{var}(h_x^2 \gamma_x(\mathcal{S})) \quad (30)$$

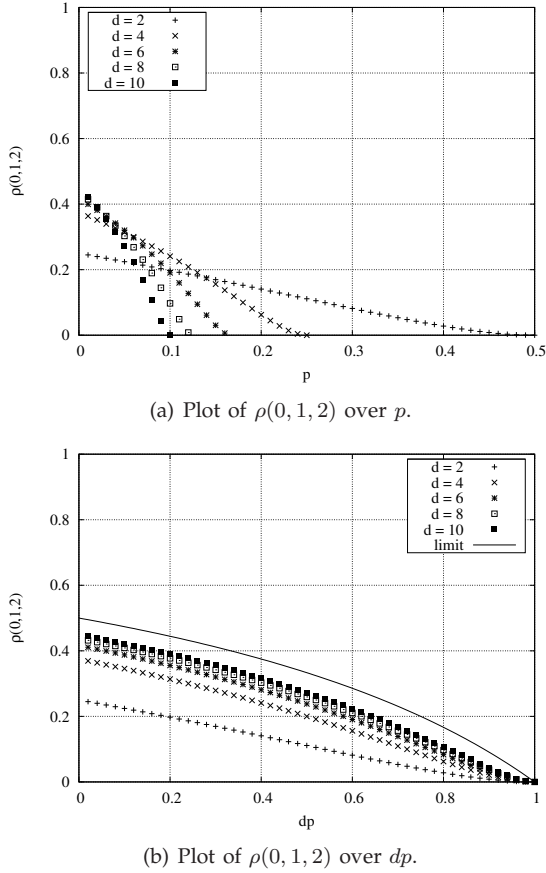


Fig. 2. Interference correlation in case $(0, 1, 2)$.

with

$$\begin{aligned} \text{var}(h_x^2 \gamma_x(\mathcal{S})) &= \mathbb{E}[h_x^4 \gamma_x^2(\mathcal{S})] - (\mathbb{E}[h_x^2 \gamma_x(\mathcal{S})])^2 \\ &= 2dp - (dp)^2 \end{aligned} \quad (31)$$

for a node x , which yields

$$\mathbb{E}[\text{var}(I(\mathcal{S}) | \mathcal{N})] \stackrel{\alpha \geq 2}{\approx} \kappa^2 \cdot \lambda \frac{\alpha\pi}{\alpha-1} \cdot dp(2-dp). \quad (32)$$

The resulting correlation coefficient

$$\rho(0, 1, 2) = \frac{(d-1)(dp-1)^2}{d(p(d-1)-1)(dp-2)} \quad (33)$$

is plotted in Figure 2. The qualitative behavior is similar to that of case $(0, 0, 2)$. The correlation coefficient is approximately halved, as the interference variance is approximately doubled—compare (28) and (32). The correlation increases for very large messages and approaches $\lim_{d \rightarrow \infty} \rho(0, 1, 2) = \frac{p-1}{p-2}$. This upper bound is also depicted in Figure 2(b).

3.6 Correlation Caused by Node Positions and Traffic; Cases $(2, j, 2)$, $j = 0, 1$

Again we partition the senders of each slot into \mathcal{S}_{11} , \mathcal{S}_{10} , and \mathcal{S}_{01} . The expected fractions of nodes in these sets are

the same as in cases $(0, 0, 2)$ and $(0, 1, 2)$; they are given in (18) and (19). Our goal is to derive

$$\rho(2, j, 2) = \frac{\text{cov}(I_{11} + I_{10}, I_{11} + I_{01})}{\text{var}(I(\mathcal{S}))}. \quad (34)$$

First, we derive the covariance of the interference values in the time slots $(t-1)$ and t . To do so, we compute

$$\begin{aligned} \mathbb{E}[(I_{11} + I_{10})(I_{11} + I_{01})] &= \\ &= \mathbb{E}\left[\sum_{x \in \mathcal{S}_{11} \cup \mathcal{S}_{10}} \kappa l(\|x\|) h_x^2 \cdot \sum_{y \in \mathcal{S}_{11} \cup \mathcal{S}_{01}} \kappa l(\|y\|) h_y^2\right] \\ &= \mathbb{E}\left[\sum_{x \in \mathcal{S}_{11}} \kappa^2 l^2(\|x\|) h_x^4\right] \\ &\quad + \mathbb{E}\left[\sum_{\substack{x \in \mathcal{S}_{11} \cup \mathcal{S}_{10} \\ y \in \mathcal{S}_{11} \cup \mathcal{S}_{01} \\ x \neq y}} \kappa^2 l(\|x\|) l(\|y\|) h_x^2 h_y^2\right] \\ &= \kappa^2 \left(p(d-1) + \frac{p^2}{1-p(d-1)}\right) \lambda \int_{\mathbb{R}^2} l^2(\|x\|) dx \\ &\quad + \left(\kappa dp \lambda \int_{\mathbb{R}^2} l(\|x\|) dx\right)^2 \\ &\stackrel{\alpha \geq 2}{\approx} \kappa^2 \left(p(d-1) + \frac{p^2}{1-p(d-1)}\right) \lambda \frac{\alpha\pi}{\alpha-1} \\ &\quad + \left(\kappa dp \lambda \frac{\alpha\pi}{\alpha-2}\right)^2. \end{aligned} \quad (35)$$

$$\quad (36)$$

Furthermore, it follows from (10) that

$$\mathbb{E}[I_{11} + I_{10}] = \mathbb{E}[I_{11} + I_{01}] \stackrel{\alpha \geq 2}{\approx} \kappa dp \lambda \frac{\alpha\pi}{\alpha-2}. \quad (37)$$

Using (1) yields

$$\begin{aligned} \text{cov}(I_{11} + I_{10}, I_{11} + I_{01}) &= \\ &= \mathbb{E}[(I_{11} + I_{10})(I_{11} + I_{01})] - \mathbb{E}[I_{11} + I_{10}] \mathbb{E}[I_{11} + I_{01}] \\ &\stackrel{\alpha \geq 2}{\approx} \kappa^2 \left(p(d-1) + \frac{p^2}{1-p(d-1)}\right) \lambda \frac{\alpha\pi}{\alpha-1}. \end{aligned} \quad (38)$$

Next, we derive the interference variance, using an approach similar to that of [10]. The second moment of the interference is

$$\begin{aligned} \mathbb{E}[I^2(\mathcal{S})] &= \mathbb{E}\left[\left(\sum_{x \in \mathcal{S}} \kappa l(\|x\|) h_x^2\right)^2\right] \\ &= \mathbb{E}\left[\sum_{x \in \mathcal{S}} \kappa^2 l^2(\|x\|) h_x^4\right] \\ &\quad + \mathbb{E}\left[\sum_{x, y \in \mathcal{S}} \kappa^2 l(\|x\|) l(\|y\|) h_x^2 h_y^2\right] \\ &= \mathbb{E}[h^4] \kappa^2 dp \lambda \int_{\mathbb{R}^2} l^2(\|x\|) dx \\ &\quad + \left(\kappa dp \lambda \int_{\mathbb{R}^2} l(\|x\|) dx\right)^2 \\ &\stackrel{\alpha \geq 2}{\approx} \mathbb{E}[h^4] \kappa^2 dp \lambda \frac{\alpha\pi}{\alpha-1} + \left(\kappa dp \lambda \frac{\alpha\pi}{\alpha-2}\right)^2. \end{aligned} \quad (39)$$

$$\quad (40)$$

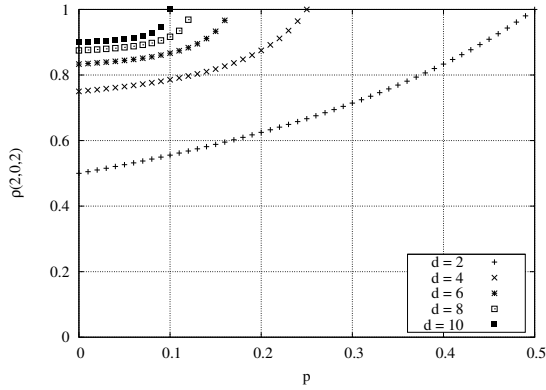


Fig. 3. Interference correlation in case $(2, 0, 2)$.

The variance is thus

$$\begin{aligned} \text{var}(I(S)) &= \mathbb{E}[I^2(S)] - (\mathbb{E}[I(S)])^2 \\ &\stackrel{\alpha \geq 2}{=} \mathbb{E}[h^4] \kappa^2 dp \lambda \frac{\alpha \pi}{\alpha - 1}. \end{aligned} \quad (41)$$

Dividing (38) by (41) yields the correlation coefficient

$$\rho(2, j, 2) = \frac{d - 1 + \frac{p}{1 - p^{(d-1)}}}{d \mathbb{E}[h^4]} \quad \text{for } j = 0, 1 \quad (42)$$

with $\mathbb{E}[h^4] = 1$ for nonfading channels ($j = 0$) and $\mathbb{E}[h^4] = 2$ for Rayleigh fading ($j = 1$).

As shown in Figure 3, the correlation in a nonfading channel increases for increasing p and d . The curves can roughly be interpreted as a blend of the cases $(0, 0, 2)$ and $(2, 0, 1)$: The correlation for p being almost zero is similar to case $(0, 0, 2)$, as $\rho(2, 0, 1)$ is equal to the fraction dp of sending nodes. When increasing p , the correlation caused by the traffic decreases, but the correlation caused by the node locations increases linearly with dp . Ultimately, when $dp \rightarrow 1$, the curves approximate the linear function dp . When messages are very long, the correlation approaches one, i.e., $\lim_{d \rightarrow \infty} \rho(2, 0, 2) = 1$ for given dp .

When Rayleigh fading is considered, the variance is doubled, as can be observed in (41). Hence, the correlation coefficient is halved, i.e. $\rho(2, 1, 2) = \frac{\rho(2, 0, 2)}{2}$. The limit for $d \rightarrow \infty$ is also halved, i.e. $\lim_{d \rightarrow \infty} \rho(2, 1, 2) = \frac{1}{2}$. A plot of $\rho(2, 1, 2)$ is not shown.

3.7 Correlation Caused by Fading under Constant Traffic; Cases $(0, 2, 0)$, $(2, 2, 0)$.

We now study the effects of a dependent fading channel on interference correlation under constant traffic. Recall that the channel state of each node changes after $c \geq 2$ slots. These changes are independent for each node, i.e., they are not synchronized.

In case $(0, 2, 0)$, the sending nodes are preselected and do not change. In each pair of slots, the expected fraction of nodes changing their channel state is $1/c$. The interference of these nodes is uncorrelated. The interference correlation of all other nodes, which perceive the

same channel state in both slots, is 1. Hence, the overall correlation is

$$\rho(0, 2, 0) = \frac{c - 1}{c}. \quad (43)$$

In case $(2, 2, 0)$, the correlation caused by the locations is also considered. The expected fraction of senders with a channel change is again $1/c$. The interference correlation of these senders is $1/2$, similar to case $(2, 1, 0)$. The interference correlation of nodes with the same channel state is 1, as derived for case $(2, 0, 0)$. Overall, we can compute the interference correlation as a weighted sum of these two cases by $\frac{1}{2c} + (1 - \frac{1}{c})$, which yields

$$\rho(2, 2, 0) = \frac{2c - 1}{2c}. \quad (44)$$

3.8 Correlation Caused by Fading under Random Traffic; Cases $(2, 2, 1)$ and $(0, 2, 1)$.

This section addresses a dependent Rayleigh fading channel under random traffic with static nodes.

3.8.1 Node positions are not given

The case $(2, 2, 1)$ can be interpreted as a combination of $(2, 0, 1)$ and $(2, 1, 1)$. Recall that \mathcal{S}_{11} contains all nodes sending in both slots, and a subset $\mathcal{S}'_{11} \subset \mathcal{S}_{11}$ of them have the same channel state in both slots. The nodes \mathcal{S}'_{11} cause a correlation of p similar to case $(2, 0, 1)$; the other nodes cause a correlation of $p/2$ similar to case $(2, 1, 1)$. Using the fraction $S_c := \mathcal{S}'_{11}/\mathcal{S}_{11}$, the correlation is

$$\rho(2, 2, 1) = \mathbb{E}[S_c] p + (1 - \mathbb{E}[S_c]) \frac{p}{2}. \quad (45)$$

Next, we derive an expression for $\mathbb{E}[S_c]$. Recall that the channel state changes after c slots. The details of our model are as follows. The number of slots between a given slot τ and the next change of the channel state is called $c_\tau \in \{0, \dots, c\}$ for a given node. When a node sends for the first time, the counter c_τ is set to c . It is reduced in each slot, independent of whether or not messages are sent, and approaches 1 after c slots. If the node immediately sends another message, the counter will be reset to c . If the node does not immediately send another message, the counter will approach 0, remain at this level, and be reset to c at the beginning of the next message. With this model, there is a channel state change between slot $(t - 1)$ and t if and only if $c_{t-1} = 1$, which means that $\mathbb{E}[S_c] = 1 - \mathbb{P}(c_{t-1} = 1)$. This probability can be computed by combining the following three facts:

- 1) The sum of the probabilities of all possible values for c_{t-1} gives 1, i.e. $\sum_{n=0}^c \mathbb{P}(c_{t-1} = n) = 1$.
- 2) If c_τ has the value c , it afterwards also takes the values $c - 1, \dots, 1$. Thus, $\mathbb{P}(c_{t-1} = 1) = \mathbb{P}(c_{t-1} = 2) = \dots = \mathbb{P}(c_{t-1} = c)$.
- 3) In order for c_{t-1} to take the value c , it is either 0 or 1 in slot $(t - 2)$ and the node has to send, i.e. $\mathbb{P}(c_{t-1} = c) = p(\mathbb{P}(c_{t-2} = 0) + \mathbb{P}(c_{t-2} = 1))$.

Combining these properties yields

$$\mathbb{P}(c_{t-1} = 1) = 1 - \mathbb{E}[S_c] = \frac{p}{1 + (c - 1)p}, \quad (46)$$

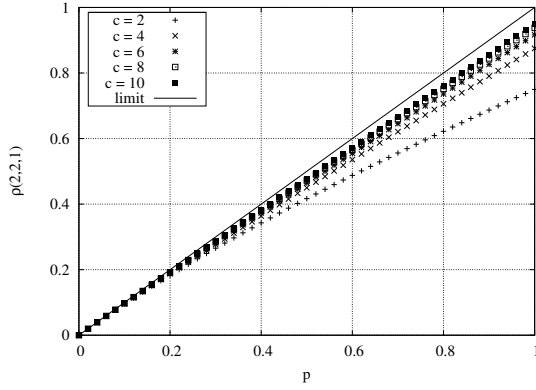


Fig. 4. Interference correlation in case (2, 2, 1).

which can be employed in (45).

Figure 4 shows the resulting interference correlation

$$\rho(2, 2, 1) = \frac{p}{2} \left(2 - \frac{p}{1 + (c-1)p} \right) \quad (47)$$

for different values of p and c . The interference becomes more correlated for increasing traffic and slower fading. We have a very similar situation as in case (2, 0, 1), where no fading occurs but the channel stays constant all the time. The limiting value is given by $\lim_{c \rightarrow \infty} \rho(2, 2, 1) = p$.

3.8.2 Node positions are given

Let us now turn to case (0, 2, 1). For given node positions \mathcal{N} , the correlation coefficient is, in general, given by the right hand side of (15). Using the sender subsets $\mathcal{S}'_{11} \cup \mathcal{S}''_{11} = \mathcal{S}_{11}$ and their interference values $I'_{11} + I''_{11} = I_{11}$, the enumerator is

$$\begin{aligned} \mathbb{E}[\text{cov}(I'_{11} + I''_{11} + I_{10}, I'_{11} + I''_{11} + I_{01} | \mathcal{N})] &= \quad (48) \\ &= \mathbb{E}[\text{var}(I'_{11} | \mathcal{N})] + 2 \mathbb{E}[\text{cov}(I'_{11}, I''_{11} | \mathcal{N})] \\ &\quad + \mathbb{E}[\text{var}(I''_{11} | \mathcal{N})] + 2 \mathbb{E}[\text{cov}(I'_{11}, I_{10} | \mathcal{N})] \\ &\quad + 2 \mathbb{E}[\text{cov}(I''_{11}, I_{10} | \mathcal{N})] + \mathbb{E}[\text{cov}(I_{10}, I_{01} | \mathcal{N})]. \end{aligned}$$

These covariances can be calculated by (17), which requires the corresponding correlation coefficients and variances. With random independent traffic, a node becomes sender with probability p in a given slot. We have $\mathbb{E}[S_{11}] = p^2$ and $\mathbb{E}[S_{10}] = \mathbb{E}[S_{01}] = p - p^2$. The nodes in \mathcal{S}_{11} are split into two subgroups of size $\mathbb{E}[S'_{11}] = p^2 \mathbb{E}[S_c]$ and $\mathbb{E}[S''_{11}] = p^2 (1 - \mathbb{E}[S_c])$, where S_c is again the fraction of nodes in \mathcal{S}_{11} that have the same channel state in both slots and is given by (46). Using these expected values in Theorem 1, we can derive the correlations $\rho(I_{11}, I''_{11})$, $\rho(I'_{11}, I_{10})$, $\rho(I''_{11}, I_{10})$, and $\rho(I_{10}, I_{01})$. Using these values in (23) with (22), we can derive the expected variances $\mathbb{E}[\text{var}(I'_{11} | \mathcal{N})]$, $\mathbb{E}[\text{var}(I''_{11} | \mathcal{N})]$, $\mathbb{E}[\text{var}(I_{10} | \mathcal{N})]$, and $\mathbb{E}[\text{var}(I_{01} | \mathcal{N})]$. Note that these variances are calculated without considering fading, since fading does not change the covariances, as shown in Theorem 2. Results are given in Appendix B and can be applied in (48).

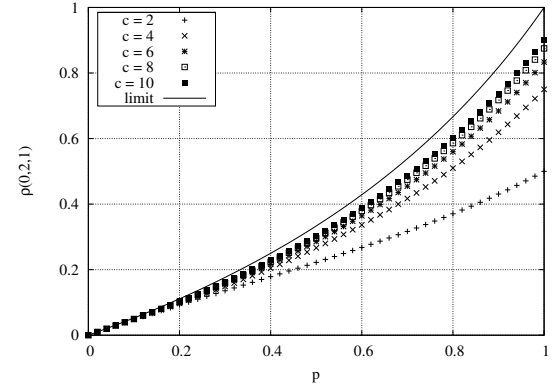


Fig. 5. Interference correlation in case (0, 2, 1).

Finally, the correlation coefficient is obtained by dividing (48) by (32) with $d = 1$, which yields

$$\rho(0, 2, 1) = \frac{p(1 + p(c-2))}{(2-p)(1 + p(c-1))}. \quad (49)$$

Figure 5 shows that the interference correlation in this case increases with increasing traffic and decreases with the rapidity of fading. Asymptotically, we have $\lim_{c \rightarrow \infty} \rho(0, 2, 1) = \frac{p}{2-p}$. Comparing Figures 4 and 5, the correlation coefficient is higher in case (2, 2, 1) for given c and p , since in that case the node locations are an additional source of correlation.

3.9 Correlation Caused by Fading and Traffic; Case (0, 2, 2).

The temporal correlation of interference in case (0, 2, 2) has two sources: fading and traffic. These sources strongly depend on each other and cannot be analyzed individually. As in case (0, 0, 2), the expected fraction of nodes in \mathcal{S}_{11} , \mathcal{S}_{10} , and \mathcal{S}_{01} is given in (18) and (19). Recall that the nodes \mathcal{S}'_{11} have the same channel state in both slots, and the nodes \mathcal{S}''_{11} have different states.

The major task is to determine $\mathbb{E}[S''_{11}]$, which also enables us to compute $\mathbb{E}[S'_{11}] = \mathbb{E}[S_{11}] - \mathbb{E}[S''_{11}]$. The number of slots from a certain slot τ to the next channel state change is again called $c_\tau \in \{0, \dots, c\}$ for a given node. The probability that the regarded slots $(t-1)$ and t have different channel states is $\mathbb{P}(c_{t-1} = 1)$. We compute the joint probability that a node x transmits in both slots and the channel state changes after the first slot, i.e.,

$$\mathbb{E}[S''_{11}] = \mathbb{P}((x \in \mathcal{S}_{11}) \wedge (c_{t-1} = 1)). \quad (50)$$

The value of c_{t-1} is determined by the transmission history of the node, i.e., by the sequences of empty and nonempty slots of this node before slot $(t-1)$. It is, however, not necessary to consider the full history but only back to until a block of $(c-1)$ consecutive empty slots. This analysis is sufficient as c_τ is equal to zero after $(c-1)$ consecutive empty slots independent of the node's previous traffic. Hence, we have to find all possible

sequences after a block of $(c - 1)$ consecutive empty slots that lead to $c_{t-1} = 1$. For each of these sequences, we calculate its occurrence probability. Summing up all these probabilities yields (50).

All possible sequences can be built up by concatenating the following building blocks: a message of duration d , a message of duration d followed by one empty slot, \dots , a message of length d followed by $(c - 2)$ empty slots. Each of these blocks can be identified by its length in terms of slots modulo c . This identification (ID) is unique for given c and d , and it is equal to the change of c_τ during the block. Let \mathcal{B} denote the set of all blocks (IDs) appearing for given c and d . The probability of occurrence for a given block with ID $m \in \mathcal{B}$ is $p(1 - p)^{(m-d) \bmod c}$. Table 2 shows the block lengths, probabilities of occurrence, and IDs.

TABLE 2
Blocks for traffic behavior.

Block length	d	$d + 1$	\dots	$d + c - 2$
Probability	p	$p(1 - p)$	\dots	$p(1 - p)^{c-2}$
Block ID	$d \bmod c$	$d + 1 \bmod c$	\dots	$d + c - 2 \bmod c$

Each sequence consists of one or more blocks. Next, we try to find sequences (m_i) that have some desired properties, where $m_i \in \mathcal{B}$ for all indices i . Let $|m_i|$ denote the length of (m_i) in terms of blocks and $\|m_i\|$ its length in terms of slots. Then we have

$$\|m_i\| := \sum_{i=1}^{|m_i|} d + (m_i - d \bmod c). \quad (51)$$

Furthermore, let \mathcal{M} denote the set of all possible sequences (m_i) . The probability of occurrence of a sequence is denoted by $\mathbb{P}(m_i)$. A sequence (m_i) is called an (s, e) -sequence, if $c_\tau = s$ at the beginning of the sequence implies $c_{j+\|m_i\|} = e$ at the end of the sequence. The set of all (s, e) -sequences can be defined as

$$\mathcal{M}(s, e) := \left\{ (m_i) \in \mathcal{M} : s + \sum_{i=1}^{|m_i|} m_i \equiv e \pmod{c} \right\}. \quad (52)$$

A minimal (s, e) -sequence is a sequence (m_i) for which no subsequence $(m_j)_{j \in I \subsetneq \{1, \dots, |m_i\}}$ is an (s, e) -sequence. The set of all minimal (s, e) -sequences is

$$\mathcal{M}^1(s, e) := \left\{ (m_i) \in \mathcal{M}(s, e) : s + \sum_{i \in I} m_i \not\equiv e \pmod{c} \right. \\ \left. \forall I \subsetneq \{1, \dots, |m_i|\}, I \neq \emptyset \right\}. \quad (53)$$

Such a minimal sequence has a length of at most $|m_i| \leq c + 1$. To proof this fact, we assume for a moment $|m_i| > c + 1$. Since $0 \leq c_\tau \leq c$, c_τ has the same value in at least two different slots. If we remove the subsequence inbetween these two slots, we get a subsequence that is again an (s, e) -sequence, which is a contradiction.

The probability that the sequence of a node is a minimal (s, e) -sequence is

$$\begin{aligned} \mathbb{P}(\mathcal{M}^1(s, e)) &= \sum_{(m_i) \in \mathcal{M}^1(s, e)} \prod_{j=1}^{|m_i|} p(1 - p)^{(m_i - d) \bmod c} \\ &= \sum_{(m_i) \in \mathcal{M}^1(s, e)} p^{|m_i|} (1 - p)^{\sum_{j=1}^{|m_i|} (m_i - d) \bmod c}. \end{aligned} \quad (54)$$

A (minimal) neutral sequence regarding s is a (minimal) (s, s) -sequence. The probability of occurrence of all neutral sequences regarding s can be derived from the occurrence probability of the minimal (s, s) -sequences as the sum of the infinite geometric series:

$$\mathbb{P}(\mathcal{M}(s, s)) = \sum_{i=0}^{\infty} \mathbb{P}(\mathcal{M}^1(s, s))^i = \frac{1}{1 - \mathbb{P}(\mathcal{M}^1(s, s))}. \quad (55)$$

This expression does, however, not hold for probabilities $\mathbb{P}(\mathcal{M}(s, e))$ with $s \neq e$. To compute those probabilities, we first have to introduce another concept: Let $\mathcal{M}^1(s, s, \mathcal{E}) \subseteq \mathcal{M}^1(s, s)$ with $\mathcal{E} \subset \mathcal{B}$ denote the set of all minimal neutral sequences regarding s in which the values in \mathcal{E} never occur for c_τ , i.e.

$$\begin{aligned} \mathcal{M}^1(s, s, \mathcal{E}) &:= \left\{ (m_i) \in \mathcal{M}^1(s, s) : s + \sum_{j=1}^k m_i \not\equiv e \pmod{c} \right. \\ &\quad \left. \forall e \in \mathcal{E}, 1 \leq k \leq |m_i| \right\}. \end{aligned} \quad (56)$$

We can construct $\mathcal{M}(s, e)$ with $s \neq e$ in the following way: Take a sequence $(m_i) \in \mathcal{M}^1(s, e)$ and place neutral sequences regarding c_τ between each two blocks as well as at the beginning and end. Neutral sequences in which a value for c_τ occurs that previously occurred within the sequence under consideration are excluded from this placement, since otherwise the resulting sequence would contain neutral subsequences other than the ones inserted. Hence the construction process would not be unique for each sequence, i.e., we could construct the same sequence out of two different elements in $\mathcal{M}^1(s, e)$.

Furthermore, let $C(s, (m_i), r)$ denote the value of c_{j+r} at position r of the sequence (m_i) with $c_\tau = s$, i.e.

$$C(s, (m_i), r) := s + \sum_{i=1}^r m_i \pmod{c}, \quad (57)$$

and $C(s, (m_i), 0) := s$. Let $(m_i)_l$ denote the l th element of a list of sequences. Two sequences (m_i) and (m'_j) are concatenated by writing $(m_i) \cup (m'_j)$. In mathematical terms, the set $\mathcal{M}(s, e)$ with $s \neq e$ can be constructed as

$$\begin{aligned} \mathcal{M}(s, e) &= \left\{ (m_i)_0 \cup \bigcup_{k=1}^{|m'_j|} (m'_k \cup (m_i)_k) : \right. \\ &\quad \forall (m'_j) \in \mathcal{M}^1(s, e), \\ &\quad \left. \forall (m_i)_k \in \mathcal{M}^1 \left(C(s, (m'_j), k), C(s, (m'_j), k), \right. \right. \\ &\quad \left. \left. \{ C(s, (m'_j), o) \mid \forall 0 \leq o \leq k - 1 \} \right) \right\}. \end{aligned} \quad (58)$$

Hence, the probability that the given sequence is part of $\mathcal{M}(s, e)$ with $s \neq e$ is given by

$$\mathbb{P}(\mathcal{M}(s, e)) = \sum_{(m_i) \in \mathcal{M}^!(s, e)} \mathbb{P}(m_i) \prod_{j=0}^{|m_i|} \mathbb{P}\left(\mathcal{M}^!(C(s, (m_i), j), C(s, (m_i), j), \{C(s, (m_i), o) \mid \forall 0 \leq o \leq j-1\})\right). \quad (59)$$

The probability $\mathbb{P}(\mathcal{M}(0, e))$ can be interpreted as the probability that $c_\tau = e$ occurs.

As mentioned in (50), we are interested in the probability that a node sends in both slots $(t-1)$ and t and that $c_{t-1} = 1$. This comprises several situations: A message could start in slot $(t-1)$ with $c_{t-1} = 1$, or in up to $(d-1)$ slots before with $c_{t-d} = (d-1 \bmod c) + 1$. In all cases, the values for c_τ are such that $c_{t-1} = 1$. In the last mentioned case, a message ends in slot $(t-1)$, so it has to be ensured that the node indeed sends a (new) message in slot t .

In summary, to compute $\mathbb{E}[S''_{11}]$, we sum over all probabilities of occurrence of these situations, with the last one multiplied with the probability that the node sends in slot t . This sum is multiplied with the probability that the block of $(c-1)$ empty slots indeed occurs and the node sends afterwards. This yields

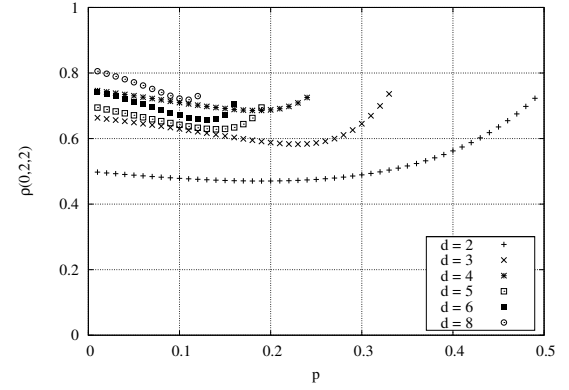
$$\mathbb{E}[S''_{11}] = p(1-p)^{c-1} \left(\sum_{i=1}^{d-1} \mathbb{P}(\mathcal{M}(0, (i-1 \bmod c) + 1)) + \mathbb{P}(\mathcal{M}(0, (d-1 \bmod c) + 1)) \frac{p}{1 - (d-1)p} \right). \quad (60)$$

Since we now know the values for $\mathbb{E}[S'_{11}]$, $\mathbb{E}[S''_{11}]$, $\mathbb{E}[S_{10}]$, and $\mathbb{E}[S_{01}]$, we can apply Theorem 1 to compute the covariances between these sets. Using the right hand side of (15) and variance (32), the correlation coefficient yields

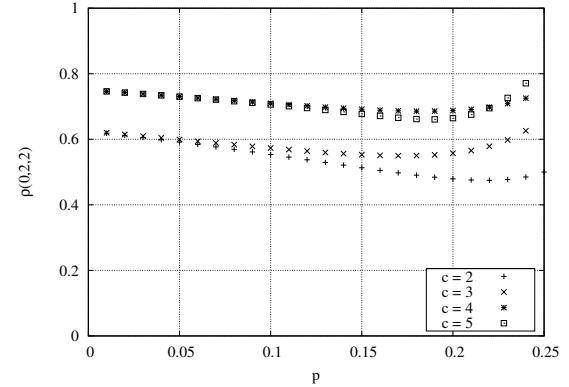
$$\rho(0, 2, 2) \stackrel{\alpha \geq 2}{=} \frac{\mathbb{E}[\text{cov}(I'_{11} + I''_{11} + I_{10}, I'_{11} + I''_{11} + I_{01} | \mathcal{N})]}{\kappa^2 \lambda \frac{\alpha \pi}{\alpha - 1} (2dp - (dp)^2)}. \quad (61)$$

Figure 6(a) shows $\rho(0, 2, 2)$ over p for different values of the message duration and a fixed channel parameter $c = 4$. Note that the curves end at $pd = 1$. The correlation is higher for longer and more overlapping messages, with the following exception: When d is an integer multiple of c , the messages and channel states synchronize, i.e., a new channel state occurs for each new message. This is the reason why increasing d from 3 to $c = 4$ yields a correlation gain, while increasing d further to 5 results in a correlation loss. For small values of dp , the slight decrease of correlation with increasing traffic is due to the decrease of the correlation caused by traffic, as can be observed in case $(0, 0, 2)$. For high dp , the correlation introduced by the channel is larger than this decrease, and hence the overall interference experiences a higher correlation.

The dependence on fading rapidity is depicted in Figure 6(b). The correlation is typically higher for slower



(a) Plot of $\rho(0, 2, 2)$ for different d with $c = 4$.



(b) Plot of $\rho(0, 2, 2)$ for different c with $d = 4$.

Fig. 6. Interference correlation in case $(0, 2, 2)$.

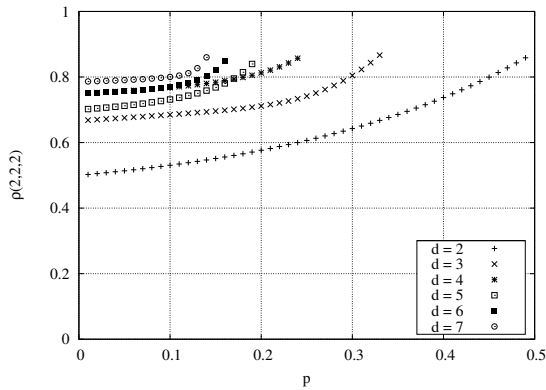
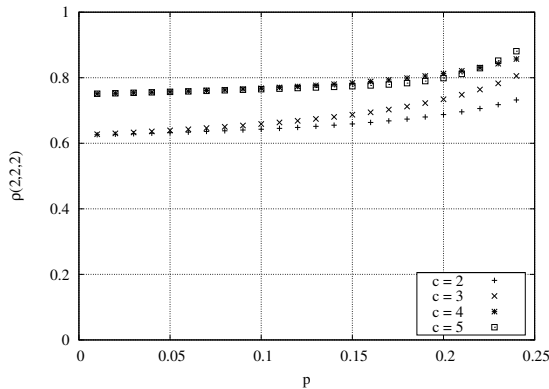
fading, except for the synchronized behavior of channel and messages explained above. The curves can be partitioned into groups, where the major increase of correlation is determined by the integer value $\lfloor \frac{c}{d} \rfloor$. A significant increase of the correlation can be observed every time c is an integer multiple of d .

3.10 Correlation Caused by Node Positions, Fading, and Traffic; Case $(2, 2, 2)$.

Case $(2, 2, 2)$ is a mixture of $(0, 2, 2)$ and $(2, 1, 2)$. The expected fraction of nodes in \mathcal{S}_{10} , \mathcal{S}_{01} , \mathcal{S}'_{11} , and \mathcal{S}''_{11} is given by case $(0, 2, 2)$. The derivation of the covariance is similar to case $(2, 1, 2)$ with the extension that the \mathcal{S}_{11} must be split into its subsets \mathcal{S}'_{11} and \mathcal{S}''_{11} . This results in

$$\begin{aligned} \text{cov}(I'_{11} + I''_{11} + I_{10}, I'_{11} + I''_{11} + I_{01}) &= \\ &= \mathbb{E}[h^4 S'_{11} + S''_{11}] \lambda \kappa^2 \int_{\mathbb{R}^2} l^2(\|x\|) dx \\ &+ (\mathbb{E}[S_{10}] - dp) \lambda^2 \left(\int_{\mathbb{R}^2} l(\|x\|) dx \right)^2 \quad (62) \end{aligned}$$

$$\begin{aligned} \stackrel{\alpha \geq 2}{=} &\mathbb{E}[h^4 S'_{11} + S''_{11}] \lambda \kappa^2 \frac{\alpha \pi}{\alpha - 1} \\ &+ (\mathbb{E}[S_{10}] - dp) \lambda^2 \left(\frac{\alpha \pi}{\alpha - 2} \right)^2. \quad (63) \end{aligned}$$

(a) Plot of $\rho(2, 2, 2)$ for different d with $c = 4$.(b) Plot of $\rho(2, 2, 2)$ for different c with $d = 4$.Fig. 7. Interference correlation in case $(2, 2, 2)$.

The corresponding correlation coefficient is

$$\rho(2, 2, 2) \stackrel{\alpha \geq 2}{=} \frac{(63)}{2dp\lambda\kappa^2 \frac{\alpha\pi}{\alpha-1}}. \quad (64)$$

As in case $(0, 2, 2)$, the correlation depends on p , c , and d . Figure 7(a) shows that the correlation increases with increasing message durations. Exceptions occur again when messages and channel states synchronize. Figure 7(b) shows the impact of fading rapidity on interference correlation. The qualitative behavior is similar to that of case $(0, 2, 2)$.

Comparing cases $(2, 2, 2)$ and $(0, 2, 2)$, the major difference is that the correlation is higher in $(2, 2, 2)$ for given parameters. This is because the node locations are an additional source of correlation. The difference is bigger for more traffic, since the correlation caused by node locations increases with p (see Section 3.4).

4 RELATED WORK

4.1 Analytical Work on Interference Correlation

Recent work by Haenggi *et al.* is very closely related to this article. The letter [10] analyzes the temporal and spatial correlation of interference in wireless networks. It applies modeling assumptions corresponding to those

of our cases $(2, j, k)$ with $j, k \in \{0, 1\}$ investigated in Section 3.4. The article [9] studies different performance measures in random wireless networks. Analytical results are based on an “uncertainty cube,” which classifies and quantifies the network stochastics with respect to node placement, fading, and medium access protocols. The results of these papers are also explained in [11].

The article at hand can be considered as a logical continuation and extension of these publications.

4.2 Analytical Work on Expected Interference

Several researchers proposed interference models for random wireless networks. Recent publications include the following. Rickenbach *et al.* [18] present a receiver-centric model of interference. Modeling the network as a disk graph, interference is determined as the number of disks overlapping the regarded receiver. Based on this model, an approximation of the optimal connectivity-preserving topology in a highway model is derived.

Dousse *et al.* [19] study the impact of interference on the connectivity of large-scale wireless multihop networks. The total interference is modeled as the weighted sum of individual interference levels and the background noise. That paper shows that, for small enough weighting factors, spatial node densities exist for which the network contains a large cluster of nodes, enabling distant nodes to communicate via multiple hops.

Jain *et al.* [20] model the impact of interference on network performance using conflict graphs. The paper presents methods for computing lower and upper bounds on the optimal throughput for a given network and workload under the assumption that packet transmissions at the individual nodes can be finely controlled and carefully scheduled by an omnipotent central entity.

Win *et al.* [21] propose a theoretical model representing the interference in wireless networks. The model is based on general assumptions, especially a very general channel model. The authors conduct four case studies, analyzing the interference of cognitive radio networks, the interference in wireless packet networks, the spectrum of the aggregate radio-frequency emission, and the coexistence of narrowband and ultrawideband systems. A comprehensive analysis of one of these case studies, namely the coexistence of narrowband and ultrawideband systems, based on methods from stochastic geometry, is presented in [22].

All these interference models analyze only the expected interference without considering spatial and temporal correlations. Correlations are, however, of importance when assessing the performance of a wide range of communication methods.

4.3 Empirical Work on Interference Correlation

Zhu *et al.* [23] perform an empirical study on point-to-multipoint transmission. They conclude that reception events are highly correlated. It is thus not needed for

each of the neighbors to individually acknowledge reception. A protocol that reduces the number of acknowledgments is proposed and evaluated by empirical and simulation-based studies.

Srinivasan *et al.* [24] propose an empirical measure for the correlation of the successful reception for different links. They compare this measure to two commonly used empirical measures. Results show that the proposed measure performs better in terms of predicting the performance of certain protocols.

Both papers perform empirical studies on the interlink correlation of transmission success. The paper at hand provides a first step toward the goal of backing up these empirical results with a theoretical background.

5 CONCLUSIONS & RESEARCH DIRECTIONS

This article modeled and analyzed the temporal correlation of interference power in wireless networks. We considered three sources of correlation—node locations, channel, and traffic—and based the analysis on commonly-used modeling assumptions, namely homogeneously distributed nodes, Rayleigh block fading, and slotted ALOHA leading to Poisson-like traffic. Having been inspired by the work of Haenggi and Ganti, we derived equations for the correlation coefficient of the interference power in two consecutive time slots in a variety of scenarios. These equations turn into closed-form expressions for practically-relevant path loss exponents $\alpha > 2$. We also studied limiting cases for the channel coherence time and message duration approaching infinity, which provide general upper bounds.

The achieved results and used methodology clear the way for a more generalized analysis of interference correlation. A follow-up research topic is to investigate interference correlation in nonconsecutive time slots, which could serve as a tool for estimating the minimum time between two transmissions to achieve uncorrelated signal-to-interference ratios. Further extensions can be made by using more complex modeling assumptions, such as medium access control with carrier sensing or correlation caused by retransmission protocols. The ultimate goal is to derive the correlation of the outage probabilities as a function of the interference correlation. This would provide a tool for analyzing the performance of different transmission methods and protocols that fully account for the effects of interference.

ACKNOWLEDGMENTS

The authors would like to thank the six reviewers for constructive comments that helped to improve the manuscript. They would also like to thank Martin Haenggi for feedback on the authors' research. A special thanks goes to Kornelia Lienbacher for proofreading.

This work was performed in the RELAY project of the research cluster Lakeside Labs. It was partly funded by the ERDF, the Carinthian Economic Promotion Fund (KWF), and the state of Austria under grant 20214/15935/23108.

REFERENCES

- [1] M. Zorzi, R. Rao, and L. Milstein, "ARQ error control for fading mobile radio channels," *IEEE Trans. Veh. Technol.*, vol. 46, pp. 445–455, May 1997.
- [2] D. Costello, J. Hagenauer, H. Imai, and S. Wicker, "Applications of error-control coding," *IEEE Trans. Inf. Theory*, vol. 44, pp. 2531–2560, Oct. 1998.
- [3] S. Alamouti, "A simple transmit diversity technique for wireless communications," *IEEE J. Sel. Areas Commun.*, vol. 16, pp. 1451–1458, Oct. 1998.
- [4] J. Laneman, D. Tse, and G. Wornell, "Cooperative diversity in wireless networks: Efficient protocols and outage behavior," *IEEE Trans. Inf. Theory*, vol. 50, pp. 3062–3080, Dec. 2004.
- [5] X. Liu, E. Chong, and N. Shroff, "Opportunistic transmission scheduling with resource-sharing constraints in wireless networks," *IEEE J. Sel. Areas Commun.*, vol. 19, pp. 2053–2064, Oct. 2001.
- [6] G. Stüber, *Principles of Mobile Communication*. Springer, 2nd ed., 2000.
- [7] T. Feng and T. Field, "Statistical analysis of mobile radio reception: An extension of Clarke's model," *IEEE Trans. Commun.*, vol. 56, pp. 2007–2012, Dec. 2008.
- [8] L. Ahumada, R. Feick, R. Valenzuela, and C. Morales, "Measurement and characterization of the temporal behavior of fixed wireless links," *IEEE Trans. Veh. Technol.*, vol. 54, pp. 1913–1922, Nov. 2005.
- [9] M. Haenggi, "Outage, local throughput, and capacity of random wireless networks," *IEEE Trans. Wireless Commun.*, vol. 8, pp. 4350–4359, Aug 2009.
- [10] R. Ganti and M. Haenggi, "Spatial and temporal correlation of the interference in ALOHA ad hoc networks," *IEEE Commun. Letters*, vol. 13, pp. 631–633, Sept 2009.
- [11] M. Haenggi and R. Ganti, *Interference in Large Wireless Networks*. now publishing, 2009.
- [12] A. Papoulis and S. Pillai, *Probability, Random Variables and Stochastic Processes*. McGraw-Hill, 4th ed., 2002.
- [13] M. Schwartz, *Mobile Wireless Communications*. Cambridge University Press, 2005.
- [14] A. Goldsmith, *Wireless Communications*. Cambridge University Press, 2005.
- [15] L. Ozarow, S. Shamai, and A. Wyner, "Information theoretic considerations for cellular mobile radio," *IEEE Trans. Veh. Technol.*, vol. 43, pp. 359–378, May 1994.
- [16] R. Knopp and P. Humblet, "On coding for block fading channels," *IEEE Trans. Inform. Theory*, vol. 46, pp. 189–205, Jan. 2000.
- [17] N. Abramson, "The ALOHA system: Another alternative for computer communications," in *Proc. Fall Joint Comput. Conf. of the AFIPS*, vol. 37, (Houston, TX, USA), pp. 281–285, Nov. 1970.
- [18] P. Rickenbach, S. Schmid, R. Wattenhofer, and A. Zollinger, "A robust interference model for wireless ad-hoc networks," in *Proc. IEEE Intern. Paral. Distr. Proc. Symp.*, (Denver, CO, USA), Apr. 2005.
- [19] O. Dousse, F. Baccelli, and P. Thiran, "Impact of interferences on connectivity in ad hoc networks," *IEEE/ACM Trans. Netw.*, vol. 13, pp. 425–436, Apr. 2005.
- [20] K. Jain, J. Padhye, V. Padmanabhan, and L. Qiu, "Impact of interference on multihop wireless network performance," in *Proc. ACM MobiCom*, (San Diego, CA, USA), Sept. 2003.
- [21] M. Win, P. Pinto, and L. Shepp, "A mathematical theory of network interference and its applications," *Proc. IEEE*, vol. 97, pp. 205–230, Feb. 2009.
- [22] P. Pinto, A. Giorgetti, M. Win, and M. Chiani, "A stochastic geometry approach to coexistence in heterogeneous wireless networks," *IEEE J. Select. Areas Commun.*, vol. 27, pp. 1268–1282, Sept. 2009.
- [23] T. Zhu, Z. Zhong, T. He, and Z.-L. Zhang, "Exploring link correlation for efficient flooding in wireless sensor networks," in *Proc. USENIX Symp. Networked Sys. Design Implementation*, (San Jose, CA, USA), Apr. 2010.
- [24] K. Srinivasan, M. Jain, J. I. Choi, T. Azim, E. S. Kim, P. Levis, and B. Krishnamachari, "The κ factor: Inferring protocol performance using inter-link reception correlation," in *Proc. MobiCom*, (Chicago, IL, USA), Sept. 2010.

PLACE
PHOTO
HERE

Udo Schilcher studied applied computing and mathematics at the University of Klagenfurt, where he received two Dipl.-Ing. degrees with distinction (2005, 2006). Since 2005, he has been research staff member at the Networked and Embedded Systems institute at the University of Klagenfurt. His main interests are interference and node distributions in wireless networks. His doctoral thesis on inhomogeneous node distributions and interference correlation in wireless networks is expected to be awarded

with a Dr. techn. degree in 2011. He received a best paper award from the IEEE Vehicular Technology Society.

PLACE
PHOTO
HERE

Christian Bettstetter studied electrical engineering and information technology at the Technische Universität München (TUM), receiving the Dipl.-Ing. degree in 1998. He then joined the Communications Networks institute at TUM, where he was a staff member until 2003. His doctoral thesis on ad hoc networks was awarded the Dr.-Ing (summa cum laude) degree in 2004. He was then a senior researcher at DOCOMO Euro-Labs. Since 2005, Christian has been a professor and head of the Networked and Embedded Systems institute at the University of Klagenfurt, performing

research and teaching on mobile and wireless networking and self-organizing systems. He is also scientific director and founder of Lakeside Labs, a research cluster on self-organizing networked systems. He received best paper awards from the IEEE Vehicular Technology Society and the German ITG. He also co-authored the Wiley textbook *GSM - Architecture, protocols and services*.

PLACE
PHOTO
HERE

Günther Brandner studied applied computing and mathematics at the University of Klagenfurt, where he received two Dipl.-Ing. degrees with distinction (2007, 2008). Since 2007, he has been a research and teaching staff member and doctoral student at the Networked and Embedded Systems institute at the University of Klagenfurt. His main interests are relay selection methods for cooperative relaying and the implementation and evaluation of protocols on hardware platforms.

APPENDIX A THE CORRELATION BETWEEN INTERFERENCE VALUES FROM DISJOINT NODE SETS

A given set of nodes \mathcal{N} is randomly partitioned into three disjoint subsets $\mathcal{N}_1, \mathcal{N}_2, \mathcal{N}_0$. These subsets contain the fractions $N_1, N_2, 1 - N_1 - N_2$, respectively, of all nodes in \mathcal{N} . The interference caused by the nodes \mathcal{N}_1 at a given point is called $I(\mathcal{N}_1)$, the one caused by \mathcal{N}_2 is $I(\mathcal{N}_2)$.

Theorem 1: The correlation coefficient between $I(\mathcal{N}_1)$ and $I(\mathcal{N}_2)$ without fading is

$$\rho(I(\mathcal{N}_1), I(\mathcal{N}_2)) = -\sqrt{\frac{N_1 N_2}{(1 - N_1)(1 - N_2)}}. \quad (65)$$

Proof: An indicator variable $\gamma_x(\mathcal{N}_i)$ denotes whether a node x is contained in a set \mathcal{N}_i or not, i.e.,

$$\gamma_x(\mathcal{N}_i) := \begin{cases} 1 & x \in \mathcal{N}_i \\ 0 & \text{else} \end{cases}. \quad (66)$$

This variable is Bernoulli distributed with variance $N_i(1 - N_i)$. Let us use two indicator variables: $\gamma_x := \gamma_x(\mathcal{N}_1)$ and $\gamma'_x := \gamma_x(\mathcal{N}_2)$. Their covariance is

$$\text{cov}(\gamma_x, \gamma'_x) = \mathbb{E}[\gamma_x \gamma'_x] - \mathbb{E}[\gamma_x] \mathbb{E}[\gamma'_x] = 0 - N_1 N_2 \quad (67)$$

$$\text{and } \text{cov}(\gamma_x, \gamma'_y) = 0 \quad \forall x \neq y \quad (68)$$

for two different nodes x and y .

Thus, for given node locations \mathcal{N} and no fading ($h_x = 1$), the covariance of the two interference values created by the two sets can be expressed as

$$\begin{aligned} \text{cov}(I(\mathcal{N}_1), I(\mathcal{N}_2) | \mathcal{N}) &= \\ \stackrel{(5)}{=} & \text{cov} \left(\sum_{x \in \mathcal{N}} \kappa l(\|x\|) \gamma_x, \sum_{y \in \mathcal{N}} \kappa l(\|y\|) \gamma'_y \middle| \mathcal{N} \right) \\ = & \kappa^2 \sum_{x, y \in \mathcal{N}} l(\|x\|) l(\|y\|) \text{cov}(\gamma_x, \gamma'_y) \end{aligned} \quad (69)$$

$$\stackrel{(67),(68)}{=} -\kappa^2 N_1 N_2 \sum_{x \in \mathcal{N}} l^2(\|x\|). \quad (70)$$

The variance of the interference created by the first node set is

$$\begin{aligned} \text{var}(I(\mathcal{N}_1) | \mathcal{N}) &= \text{var} \left(\sum_{x \in \mathcal{N}} \kappa l(\|x\|) \gamma_x \middle| \mathcal{N} \right) \\ &= \kappa^2 \sum_{x \in \mathcal{N}} l^2(\|x\|) \text{var}(\gamma_x) \\ &= \kappa^2 N_1(1 - N_1) \sum_{x \in \mathcal{N}} l^2(\|x\|) \end{aligned} \quad (71)$$

and a similar expression for $\text{var}(I(\mathcal{N}_2) | \mathcal{N})$.

Applying (69) and (71) in (2) yields

$$\begin{aligned} \rho(I(\mathcal{N}_1), I(\mathcal{N}_2) | \mathcal{N}) &= \\ &= \frac{-\kappa^2 N_1 N_2 \sum_{x \in \mathcal{N}} l^2(\|x\|)}{\sqrt{N_1(1 - N_1)} \sqrt{N_2(1 - N_2)} \kappa^2 \sum_{x \in \mathcal{N}} l^2(\|x\|)} \\ &= -\sqrt{\frac{N_1 N_2}{(1 - N_1)(1 - N_2)}}, \end{aligned} \quad (72)$$

which is the correlation coefficient conditioned by the set of nodes \mathcal{N} . The second equation holds if the sum over all path loss values converges. Since (72) is independent of \mathcal{N} , we have $\rho(I(\mathcal{N}_1), I(\mathcal{N}_2)) = \rho(I(\mathcal{N}_1), I(\mathcal{N}_2) | \mathcal{N})$. \square

Note that the correlation (65) is negative, since the two node sets are disjoint.

Theorem 2: The covariance between $I(\mathcal{N}_1)$ and $I(\mathcal{N}_2)$ if each link experiences independent Rayleigh fading is (70), i.e., fading does not change the covariance.

Proof: Using indicator variables as defined above and the channel state h_x^2 of node x , the covariance of the indicator variables and the channel states is

$$\begin{aligned} \text{cov}(\gamma_x h_x^2, \gamma'_y h_y^2) &= \mathbb{E}[\gamma_x \gamma'_y h_x^2 h_y^2] - \mathbb{E}[\gamma_x h_x^2] \mathbb{E}[\gamma'_y h_y^2] \\ &= \begin{cases} \mathbb{E}[\gamma_x \gamma'_x h_x^4] - N_1 N_2 = -N_1 N_2 & \text{for } x = y \\ 0 & \text{else} \end{cases} \end{aligned} \quad (73)$$

This result is equal to that of (67), (68). To compute $\text{cov}(I(\mathcal{N}_1), I(\mathcal{N}_2) | \mathcal{N})$ with fading, we use (73) in (69), which again gives (70), thus proving the theorem. \square

Note that, although the covariance is not influenced by fading, the variance in general increases, leading to a smaller correlation coefficient.

APPENDIX B INTERMEDIATE RESULTS FOR CASE (0, 2, 1)

$$\begin{aligned} \rho(I_{11}, I''_{11}) &= -\sqrt{\frac{p^4 S_c (1 - S_c)}{p^4 S_c (1 - S_c) - p^2 S_c}} \\ \rho(I'_{11}, I_{10}) &= -\sqrt{\frac{p^3 (1 - p) S_c}{p^2 - p + 1 - S_c (p^4 - p^3 - p^2)}} \\ \rho(I''_{11}, I_{10}) &= -\sqrt{\frac{p^3 (1 - p) (1 - S_c)}{-p^4 + p^3 - p + 1 - S_c (p^4 - p^3 - p^2)}} \\ \rho(I_{10}, I_{01}) &= -\frac{p(1 - p)}{p^2 - p + 1} \end{aligned}$$

$$\begin{aligned} \mathbb{E}[\text{var}(I'_{11} | \mathcal{N})] &\stackrel{\alpha \geq 2}{=} \kappa^2 \lambda \frac{\alpha \pi}{\alpha - 1} \left(p^2 - \frac{p^3}{1 + (c - 1)p} \right) \\ &\quad \cdot \left(1 - p^2 - \frac{p^3}{1 + (c - 1)p} \right) \\ \mathbb{E}[\text{var}(I''_{11} | \mathcal{N})] &\stackrel{\alpha \geq 2}{=} \kappa^2 \lambda \frac{\alpha \pi}{\alpha - 1} \left(\frac{p^3}{1 + (c - 1)p} \right) \\ &\quad \cdot \left(1 - \frac{p^3}{1 + (c - 1)p} \right) \\ \mathbb{E}[\text{var}(I_{10} | \mathcal{N})] &\stackrel{\alpha \geq 2}{=} \kappa^2 \lambda \frac{\alpha \pi}{\alpha - 1} (p - p^2)(1 - p + p^2) \\ \mathbb{E}[\text{var}(I_{01} | \mathcal{N})] &= \mathbb{E}[\text{var}(I_{10} | \mathcal{N})] \end{aligned}$$